When comparing Figs. 1 and 2, it was noted that the SPL's are essentially identical but that the $G_v(f)$ in Fig. 2 exhibited more tonal characteristics. Because the $G_v(f)$ in Fig. 2 was measured with a horizontal hot-film sensor and Fig. 1 data was based on a vertical hot-film, it can be stated that circumferential components of velocity exhibit more tonal characteristics than axial velocity components. This comparison also showed that, in general, the circumferential flow was more coherent with the radiated noise than the axial flow.

The most interesting information was obtained by examining the coherence of interaction tones in Fig. 1 and 2. Coherence at frequencies of $F+R$ and $2(F+R)$ was significant in Fig. 2 but absent in Fig. 1. Since the high coherence of the direct rotor fields at F, R, $2F$, and $2R$ suggests a linear transfer function, one may assume that a linear relation applies to the interaction tones as well. Thus, the circumferential flow components are closely related to interaction tones based upon sum frequencies, whereas the axial flow fluctuations are nearly independent of those same tones.

A similar comparison can be made with interaction tones associated with difference frequencies $(F-R)$. Although the level of coherence is less, there are a number of significant coherence peaks based upon $(F-R)$ and its harmonics in Fig. 1, but there are no such significant peaks in Fig. 2. This fact indicates acoustic frequencies at $(F-R)$, and its harmonics are more related to the axial flow fluctuations than circumferential fluctuations.

Interaction tones are directional, and results obtained from acoustic measurements in the forward quadrant do not assure similar coherence with sideline acoustic signals or with measurements obtained in the downstream quadrant. Although these results are from one microphone location and one hot-film sensor location, they suggest it may be possible to use this technique to help identify sources of CRP interaction noise. The method is not limited to interaction tones, since it was also observed that coherence peaks at $F/2$ and $(R+F/2)$ existed in the case of circumferential flow but not in that of axial flow. These observations indicate that there is a relationship between the radiated sound and the directional velocity components of the flowfield measured between the rotors of counterrotating propellers. Clearly, particular interaction tones are more coherent with some velocity components than with others.

Concluding Remarks

It has been shown that coherence analysis performed between the radiated sound of counter-rotating propellers and the fluctuating components of velocity between the rotors can be used to identify the existence of noise-flow relationships in aerodynamic interaction. The association of flow components with interaction noise can be identified through peaks of coherence associated with the sums and differences of the blade-passing frequencies of the forward and aft propellers. It was also found that the magnitude of the tones in the sound or flow velocity spectra were not important in establishing significant coherence.

References

[1]Magliozzi, B., "Advanced Turboprop Noise: A Historical Review," AIAA Paper 84-2261, Oct. 1984.

[2]Bradley, A. J., "A Study of the Rotor/Rotor Interaction Tones from a Contra-rotating Propeller Driven Aircraft," AIAA Paper 86-1894, July 1986.

[3]Hanson, D. B., "Noise of Counter-rotating Propellers," *Journal of Aircraft*, Vol. 22, July 1985, pp. 609-617.

[4]Bendat, J. S. and Piersol, A. G., *Random Data: Analysis and Measurement Procedures*, 2nd ed., Wiley, New York, 1986, pp. 172-176.

On Cone Frustum Pressure Gradient Effects on Transition

Kenneth F. Stetson*
U.S. Air Force Wright Aeronautical Laboratories, Wright-Patterson Air Force Base, Ohio

Nomenclature

p = pressure, kPa (lb/in.^{2})
R = radius, cm (in.)
Re = Reynolds number
Re_{x_T} = transition Reynolds number based on conditions at the edge of the boundary layer and the surface distance from the stagnation point to the location of transition
X,S = surface distance, cm (in.)
T = temperature, K (°R)
X_{SW} = entropy-layer-swallowing distance, cm (in.)
X_T = surface distance from the stagnation point to the onset of transition, cm (in.)

Subscripts

B = base
N = nose
o = reservoir
st = model stagnation point
w = wall
∞ = freestream

Introduction

THERE is a characteristic pattern for the pressure distribution on the frustum of a sphere cone in hypersonic flow. The high-pressure gas generated by the nose-tip bow shock has a limiting expansion that is possible as it proceeds around the nose tip. The expansion continues on the frustum and is often characterized with a blast wave analogy. This region of expanding flow produces a favorable pressure gradient. Continuing down the frustum, the flow overexpands (below the equivalent sharp cone pressure) and requires a recompression (an adverse pressure gradient) to arrive at the "proper" pressure at some downstream location on the frustum. Thus, the frustum of a sphere cone in hypersonic flow has both a favorable and an adverse pressure gradient. The magnitude of these pressure gradients and the extent of the regions (in terms of S/R_N) are primarily functions of freestream Mach number and cone angle. Guidance from both stability theory and experiments suggests that a favorable pressure gradient would delay boundary-layer transition and an adverse pressure gradient would promote early transition (as compared with zero pressure gradient transition). The significance of these pressure gradients on sphere-cone transition was unknown, and this author did not know of any experiments that addressed these effects. Nose-tip bluntness experiments[1-3] provided some surprising results for the favorable pressure gradient region and some interesting possible effects of the adverse pressure gradient. As transition moved closer to the nose tip, the favorable pressure gradient became increasingly stronger, yet the transition Reynolds numbers became smaller; in some cases, they were of the same order as nose tip transition Reynolds numbers. It appeared that some other effect, stronger than the effect of the favorable pressure gradient, had taken over as the dominant parameter. Further investiga-

Received Oct. 20, 1987. This paper is declared a work of the U.S. Government and is not subject to copyright protection in the United States.

*Aerospace Engineer, High Speed Aero Performance Branch, Aeromechanics Division, Flight Dynamics Laboratory. Associate Fellow AIAA.

tions of this problem (reported in Ref. 3) disclosed that nose-tip instabilities were responsible and that transition in this initial region of the frustum could be related to nose-tip sonic point Reynolds number and nose-tip surface conditions, analogous to nose-tip transition criteria. Transition results in the adverse pressure gradient region indicated that the adverse pressure gradient might be producing a large effect on transition, and further exploration of this possibility became the motivation for this present investigation.

Results and Discussion

Previous transition experiments[1-3] found that when the nose-tip radius and the freestream unit Reynolds number were such that transition occurred at locations on the cone frustum where the entropy layer was nearly swallowed by the boundary layer, transition Reynolds numbers were greater than those obtained on a sharp cone. When unit Reynolds number or nose-tip radius was increased, the swallowing distance became larger, and transition was occurring at smaller values of X_T/X_{sw}. In this region of the entropy-layer-influenced boundary layer, large reductions in the transition Reynolds number occurred. Transition Reynolds numbers became significantly less than sharp cone values and the Re_{x_T} vs X_T/X_{sw} curve had a minimum that occurred near the end of the adverse pressure gradient. It was easy to suspect that the destabilizing effects of the adverse pressure gradient had become large enough to dominate the stabilizing effect of small nose-tip bluntness. In order to explore this aspect of transition, an axisymmetric wind-tunnel model was designed in such a manner as to eliminate the adverse pressure gradient. Based on inviscid flowfield calculations, the radial dimensions of a cone were increased by just the amount required to keep the flow from overexpanding, thus providing an axisymmetric configuration without an adverse pressure gradient. The nose tip started with a 0.51-cm (0.2-in.) spherical radius, which extended beyond the sonic point. The thin-skin model was instrumented with thermocouples and surface pressure instrumentation. Figure 1 is a sketch of the resulting configuration and the calculated pressure distribution. It can be seen that only small changes in the cone dimensions were required to eliminate the adverse pressure gradient.

The experiments were conducted in the Flight Dynamics Laboratory Mach 6 wind tunnel. This tunnel is a blowdown facility operating at a reservoir temperature of 611 K (1100°R) and a reservoir pressure range of 4827–14480 kPa (700–2100 psia), corresponding to a unit Reynolds number range of 31.8 $\times$ 10^6–99.4 $\times$ 10^6/m (9.7 $\times$ 10^6—30.3 $\times$ 10^6/ft). The test core of approximately 25.4 cm (10 in.) is produced by a contoured axisymmetric nozzle with a physical exit diameter of 31.2 cm (12.3 in.). Additional details of the wind tunnel can be found in Ref. 4. The location of boundary-layer transition was obtained from heat-transfer measurements. Heat-transfer rates were calculated from the increase in the wall temperature of the model, using standard thin-skin data reduction techniques. The model was cooled between runs so that the model surface temperature would always be the same at the start of each run [approximately 300 K (540°R)]; T_w/T_o was generally in the range 0.52–0.58.

Figure 2 compares the measured surface pressures with the design conditions [R_N = 0.51 cm (0.2 in.)]. The adverse pressure gradient was eliminated, and much of the model (where transition occurred) had a zero pressure gradient.

Figure 3 compares boundary-layer transition Reynolds numbers obtained from this present investigation with the sphere cone results of Ref. 3. If the adverse pressure gradient on the sphere cone had been responsible for the large reduction in Re_{x_T} and the minimum in the curve at X_T/X_{sw} just over 0.1, then these present data would be expected to be above the sphere cone results. That the elimination of the adverse pressure gradient did not produce larger transition Reynolds numbers but, in fact, resulted in lower transition Reynolds numbers, indicated that the adverse pressure gradient played only a very minor role. As is often the case in boundary-layer transition, several effects of varying strengths are simultaneously involved. It would appear from these results that some still unidentified effect was playing the dominant role and was responsible for the large reduction in transition Reynolds number in this region of the entropy-layer-influenced boundary layer. The identification of this effect must await further experimental investigations.

A possible explanation for the lower transition Reynolds numbers on the model without the adverse pressure gradient involves the influence of the boundary-layer history. The boundary-layer history is clearly an important aspect of transition. In order for boundary-layer disturbances to grow to a magnitude sufficient to induce transition, a considerable period of growth must occur within the upstream laminar boundary layer. Pressure gradients, and the magnitude of these gradients, should influence the rate at which the boundary-layer disturbances grow. In the process of designing

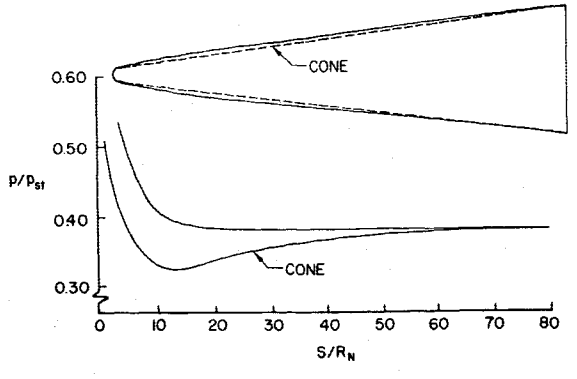

Fig. 1 Nonadverse pressure gradient model.

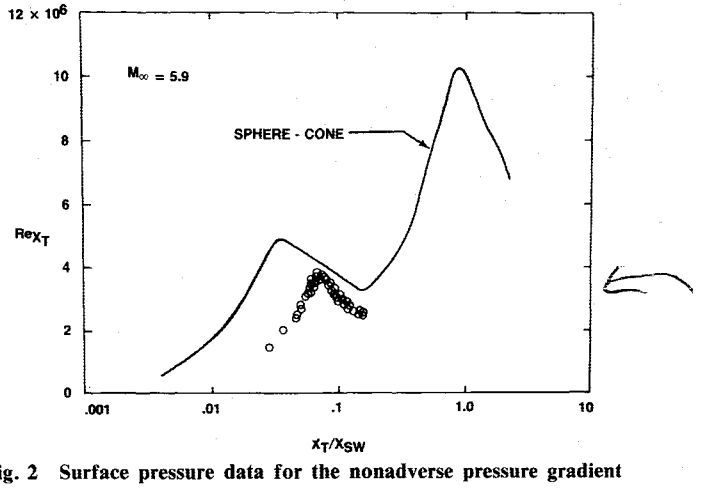

Fig. 2 Surface pressure data for the nonadverse pressure gradient model.

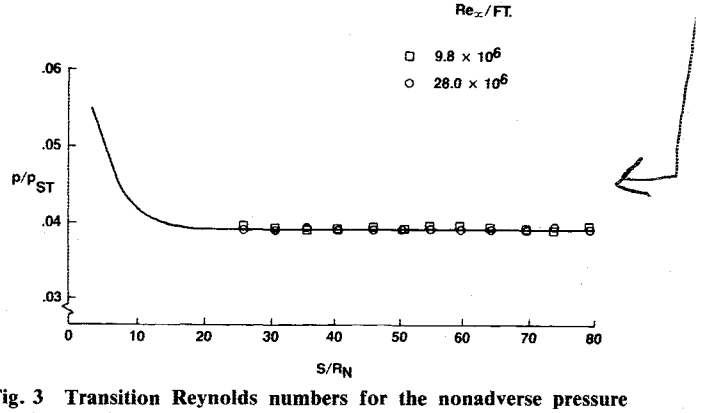

Fig. 3 Transition Reynolds numbers for the nonadverse pressure gradient model.

a model to eliminate the adverse pressure gradient, the favorable pressure gradient was made less than that of a sphere cone. Intuitively, it would be expected that a reduction in the favorable pressure gradient would result in an increase in the disturbance growth rates and an earlier transition.

These present findings have some similarity to previous shock-tube transition results, which obtained transition data both within regions of favorable pressure gradients and downstream of the gradients.[5] It was found that transition on a hemisphere configuration first occurred near the sonic point. The supersonic portion of the hemisphere always had a laminar boundary layer until transition occurred near the sonic point; at which time, the entire supersonic region would experience transition, as if the boundary layer had been tripped. This result suggested that higher transition Reynolds numbers downstream of the sonic point might be obtained on a different configuration, such as an ellipse, which had the sonic point located closer to the stagnation point. Such a configuration would have a lower Reynolds number at the sonic point than a corresponding hemisphere at the same freestream conditions and perhaps delay the "tripping" of the supersonic boundary layer. Contrary to this reasoning, transition occurred at a lower Reynolds number in the supersonic boundary layer of the ellipse than on the corresponding hemisphere. Both the ellipse and hemisphere had cylindrical aft-bodies. When transition occurred on the cylindrical portion of both configurations, it was happening within a zero pressure gradient. The cylinder preceded by an ellipse always had a lower transition Reynolds number than the cylinder preceded by a hemisphere. It was speculated that the lower transition Reynolds numbers on the ellipse-cylinder configuration were associated with the weaker favorable pressure gradient downstream of the sonic point.

Another interesting comparison of these present results was found for situations in which transition was occurring closer to the nose tip (small X_T/X_{sw}). These data correspond to the smaller values of X_T/X_{sw} of Fig. 3, where Re_{x_T} steadily decreased to low values. Reference 3 discussed the sphere cone data, where this leg of the transition curve (called "early frustum transition") corresponded to situations in which a threshold value of Reynolds number at the sonic point was exceeded and the nose-tip conditions became the dominant parameters. This special model had a spherical nose tip that extended beyond the sonic point. Therefore, the subsonic flow and the sonic point conditions for this nose tip were similar to those for the sphere cone configuration with 10% bluntness ($R_N/R_B = 0.10$). For the 10% blunt sphere cone, it was not possible to exceed the nose-tip threshold conditions and obtain early frustum transition for any test conditions. Yet the threshold conditions for this present model were easily obtained, even with a smooth nose tip. These data in Fig. 3 correspond to the left branch of the data points, which extend parallel to the sphere cone early frustum transition data. These results indicated that the early frustum transition condition depended not only on nose-tip parameters but also on the subsequent pressure gradient. This appears to be another example of the importance of boundary-layer history.

References

[1]Stetson, K. F., "Effect of Bluntness and Angle of Attack on Boundary Layer Transition on Cones and Biconic Configurations," AIAA Paper 79-0269, Jan. 1979.

[2]Stetson, K. F., "Hypersonic Boundary Layer Transition Experiments," AFWAL-TR-80-3062, Oct. 1980.

[3]Stetson, K. F., "Nosetip Bluntness Effects on Cone Frustum Boundary Layer Transition in Hypersonic Flow," AIAA Paper 83-1763, July 1983.

[4]Fiore, A. W. and Law, C. H., "Aerodynamic Calibration of the Aerospace Research Laboratories $M=6$ High Reynolds Number Facility," ARL-TR-75-0028, Feb. 1975.

[5]Stetson, K. F., "Boundary Layer Transition on Blunt Bodies With Highly Cooled Boundary Layers," *Journal of the Aerospace Sciences*, Vol. 27, Feb. 1960, pp. 81-91.

Evidence of Reynolds Number Sensitivity in Supersonic Turbulent Shocklets

J. A. Johnson III,* Y. Zhang,† and L. E. Johnson‡
The City College, New York, New York

Introduction

THE existence of turbulent shocklets in supersonic free shear layers[1] affords new phenomena in these systems. Local shock waves can alter the transport of momentum from the free shear layer into the (surrounding) ambient environment and change the mixing processes at the boundary between the free shear layer and the ambient environment. This effect might explain the anomalous behavior in the spreading rate for supersonic free shear layers;[2] indeed some speculations have already been presented that model a local shock wave's induced negative vorticity as a cause of the reduced spreading rate.[3] A local shock wave can also destroy the evolution of supersonic combustion by rendering the local flow subsonic and thereby reducing the thrust which would otherwise be available in a scramjet.[4] In all of these discussions, it has been assumed that the shocklets are the direct consequence of the existence of turbulence in the free shear layer; it is also taken for granted that the control of the strength of the shocklets has a very high priority. In this Note, we report our first clear indication of a direct connection between these shocklets and turbulence. We will also show how this connection has implications for the prospect of shocklet control.

Experiments

Our tube wind tunnel is an elaboration of the configuration originally proposed by Ludwieg.[5] A conventional shock tube is modified by the insertion of a layer-spilling asymmetric supersonic nozzle into the section upstream from the diaphragm (the high-pressure section). When the diaphragm breaks, an expansion wave moves upstream into the high-pressure section through the nozzle causing the local pressure, density, and gas velocity to change with time and as a function of distance from the location of the diaphragm. At a time determined by the ratio of the nozzle's throat area to its exit area, the nozzle is choked, i.e., the mass flow rate is frozen, and stable, steady supersonic flow is established in the exit region. The duration of this steady period is determined by the round-trip time for the head of the expansion wave to travel from the throat of the nozzle to the upstream termination (end) of the high-pressure section. When the diaphragm breaks, other wave phenomena are also produced; viz, a shock wave and a contact surface travel downstream into the low-pressure section. In the literature, one can find derivations of the formulas relating the nozzle's parameters to the initial conditions of the tube.[6] With this kind of device, high Reynolds numbers (resulting from high stagnation pressures) can be maintained in the exit region under conditions of steady supersonic flow.

The low-pressure section of our Ludwieg tube has two parts: a 6-in.-diam, 5-ft long cylindrical end piece and a 3-ft-long transition piece that changes from 6-in.-diam circular cross section to a 3.6- × 3.6-in. square at the diaphragm. The transition piece has a hand-operated plunger for rupturing the diaphragm. The high pressure section has five parts: a 6-ft-

Received Feb. 17, 1987.

*Professor, Department of Physics. Member AIAA.

†Visiting Scholar, Department of Physics. (Permanent address: College of Science Management, Chinese Academy of Sciences, Beijing, People's Republic of China.)

‡Research Associate, Department of Physics.